Acceleration Correlations and Pressure Structure Functions in High-Reynolds Number Turbulence

Haitao Xu,[1,2] Nicholas T. Ouellette,[1,2,*] Dario Vincenzi,[1,2] and Eberhard Bodenschatz[1,2,3,4,5,†]

[1]*International Collaboration for Turbulence Research*
[2]*Max Planck Institute for Dynamics and Self-Organization, D-37077 Göttingen, Germany*
[3]*Laboratory of Atomic and Solid State Physics, Cornell University, Ithaca, New York 14853, USA*
[4]*Sibley School of Mechanical and Aerospace Engineering, Cornell University, Ithaca, New York 14853, USA*
[5]*Institute for Nonlinear Dynamics, Universität Göttingen, D-37073 Göttingen, Germany*
(Received 5 August 2007; published 14 November 2007)

We present measurements of fluid particle accelerations in turbulent water flow between counter-rotating disks using three-dimensional Lagrangian particle tracking. By simultaneously following multiple particles with sub-Kolmogorov-time-scale temporal resolution, we measured the spatial correlation of fluid particle acceleration at Taylor microscale Reynolds numbers between 200 and 690. We also obtained indirect, nonintrusive measurements of the Eulerian pressure structure functions by integrating the acceleration correlations. Our measurements are in good agreement with the theoretical predictions of the acceleration correlations and the pressure structure function in isotropic high-Reynolds number turbulence by Obukhov and Yaglom in 1951 [Prikl. Mat. Mekh. **15**, 3 (1951)]. The measured pressure structure functions display $K41$ scaling in the inertial range.

Fluid particle acceleration is an important quantity in turbulent flows [1]. For example, it plays a significant role in the formation of cloud droplets in the atmosphere [2]. In recent years, advances in the study of the statistics of acceleration have been made through the development of Lagrangian experimental techniques [3,4] and the use of direct numerical simulations (see, e.g., Refs. [5–7]). Using silicon-strip detectors operating at frequencies as high as 70 kHz, La Porta and co-workers [4] were able to follow tracer particles in a water flow at Taylor microscale Reynolds numbers up to $R_\lambda \sim 10^3$. Fluid particle accelerations were obtained from the measured trajectories. Their results revealed the highly intermittent nature of acceleration and also showed the necessity of sub-τ_η temporal resolution for obtaining accurate acceleration measurements, where τ_η is the Kolmogorov time scale, the smallest time scale in turbulence. In later studies, the same technique was used to investigate the Lagrangian properties of acceleration following a fluid particle [8]. Because of the one-dimensional nature of the silicon-strip detectors, however, only one fluid particle could be followed at a time. Consequently, the spatial properties of acceleration were not explored in these previous studies. In other particle tracking experiments, digital cameras were used to record the motion of tracer particles and multiparticle statistics were obtained [9,10]. These experiments, however, were limited to flows with small R_λ because of the slower recording frequency of the cameras. Very recently, advances in camera technology have provided the opportunity of measuring the acceleration of multiple tracer particles simultaneously in high-Reynolds number turbulent flows [11]. In this Letter, we present the first direct experimental measurement of the spatial correlations of acceleration in turbulent flows with $200 \leq R_\lambda \leq 690$.

Another important quantity in high-Reynolds number turbulence that is not clearly understood is pressure. It has been shown that the clustering of inertial particles in turbulence is related to the scaling properties of the pressure field [12]. It is, however, extremely difficult to measure pressure in turbulent flows nonintrusively. Ould-Rouis *et al.* [13] reported that, in the inertial range, the pressure structure functions computed from the fourth order longitudinal velocity structure functions scale as predicted by Kolmogorov's $K41$ theory [14–16] when R_λ is moderately high ($R_\lambda \gtrsim 230$). However, Hill and Boratav [17] argued that very large Reynolds numbers are needed to observe $K41$ scaling and the assumptions made by Ould-Rouis *et al.* result in large uncertainties in the calculated pressure structure function. Pressure spectra obtained from numerical simulations [5,12,18] suggested that the $K41$ pressure spectrum can be observed only at $R_\lambda > 600$. The spectra obtained from direct pressure measurements in turbulent jets by Tsuji and Ishihara [19] seem to support this conclusion. In this experiment, however, the effect of Taylor's frozen flow hypothesis on the pressure spectra has not been fully evaluated.

In high-Reynolds number turbulence, the acceleration is mostly determined by the pressure gradient, and the viscous term may be ignored [20]. Under this assumption, there exist analytical relations between the spatial correlations of acceleration and the Eulerian pressure structure function [15,16]. By exploiting such relations, we obtain an indirect but nonintrusive measurement of the pressure structure functions in high-Reynolds number turbulence.

Our measurements are in good agreement with the predictions of Obukhov and Yaglom based on $K41$.

In high-Reynolds number flows, the spatial correlation of fluid particle acceleration is dominated by the Eulerian pressure gradient correlation. Hence,

$$R_{ij}(\mathbf{r}) \equiv \langle a_i(\mathbf{x}) a_j(\mathbf{x}+\mathbf{r}) \rangle = \frac{1}{\rho^2} \left\langle \frac{\partial p}{\partial x_i} \bigg|_\mathbf{x} \frac{\partial p}{\partial x_j} \bigg|_{\mathbf{x}+\mathbf{r}} \right\rangle. \quad (1)$$

In homogeneous, isotropic turbulence, this relation reduces to [15]

$$R_{LL}(r) = \frac{1}{2\rho^2} \frac{d^2\Pi(r)}{dr^2}, \qquad R_{NN}(r) = \frac{1}{2\rho^2} \frac{d\Pi(r)}{rdr}, \quad (2)$$

where $R_{LL}(r)$ and $R_{NN}(r)$ are the longitudinal and transverse acceleration correlations, respectively, and $\Pi(\mathbf{r}) \equiv \langle [p(\mathbf{x}+\mathbf{r}) - p(\mathbf{x})]^2 \rangle = \Pi(r)$ is the Eulerian pressure structure function. Therefore, once either $\Pi(r)$ or $R_{ij}(\mathbf{r})$ is determined, the other can also be obtained. It should be emphasized that Eqs. (2) hold in homogeneous, isotropic turbulence at high-Reynolds numbers. The only simplification invoked in deriving these equations is the neglect of a viscous contribution to acceleration.

In their work, Obukhov and Yaglom used a further assumption that the components of the velocity gradient are drawn from a multidimensional Gaussian distribution [21,22]. Under this hypothesis, $\Pi(r)$ in homogeneous, isotropic turbulence satisfies

$$\frac{d^4\Pi(r)}{dr^4} + \frac{4}{r}\frac{d^3\Pi(r)}{dr^3} = -\rho^2\Phi(r), \quad (3)$$

where $\Phi(r)$ can be written in terms of the derivatives of the longitudinal velocity structure function $D_{LL}(r)$:

$$\Phi(r) \equiv D'_{LL}\left(4D'''_{LL} + \frac{20D''_{LL}}{r} + \frac{6D'_{LL}}{r^2}\right) + 4(D''_{LL})^2. \quad (4)$$

An equation for D_{LL} can be obtained from the Kármán-Howarth equation [23] as

$$6\nu\frac{dD_{LL}}{dr} + |S|[D_{LL}(r)]^{3/2} = \frac{4}{5}\varepsilon r, \quad (5)$$

where S is the structure function skewness [24]. Obukhov and Yaglom [15] assumed that S is constant for all r, and so

it can be related to the Kolmogorov constant C_2 for the structure function $D_{LL}(r)$ as $|S| = (4/5)C_2^{-3/2}$ and the value of $C_2 = 2.13$ is well known from experiments [25]. Upon solving Eq. (5) numerically for $D_{LL}(r)$, Eq. (3) is solved for $\Pi(r)$ using Green's functions; $R_{LL}(r)$ and $R_{NN}(r)$ are then obtained from Eqs. (2).

We carried out 3D Lagrangian particle tracking (LPT) experiments in a von Kármán water flow between counter-rotating disks, as described in detail previously [11,26]. Here, we report measurements from four experiments with R_λ ranging from 200 to 690. The relevant parameters of the flow and the experiments are shown in Table I. All measurements were done in the same apparatus described in Ref. [4], except for the $R_\lambda = 460$ experiment, which was carried out in a new apparatus with a similar geometry but a different disk propeller. In the $R_\lambda = 460$ experiment, we used the Phantom v7.2 cameras from Vision Research Inc., which are capable of recording at 37 000 frames per second at a resolution of 256×256 pixels, nearly a 40% increase in frame rate compared to the v7.1 cameras used in the other experiments. Therefore, the $R_\lambda = 460$ experiment has the highest temporal resolution among the four experiments reported here.

Figure 1 compares the acceleration probability density function (PDF) measured in the $R_\lambda = 460$ experiment with the PDF measured in Ref. [28] at $R_\lambda = 690$ using silicon-strip detectors. (We note that there is possibly a weak dependence of acceleration PDF on the Reynolds number [29]. Previous experiments, however, indicate that the dependence is so small that within experimental uncertainty, the measured acceleration flatness is nearly a constant over the range $285 \le R_\lambda \le 970$ [4].) It can be seen that with a temporal resolution comparable to the silicon-strip detector measurement, where the sampling frequency is 65 frames per τ_η, the PDFs measured with cameras are in remarkable agreement with the silicon-strip detector data. Even the fourth moment agrees well, as shown in the inset to Fig. 1. The spatial resolution in the measurement with cameras, 40 μm/pixel, is significantly worse than that of the silicon-strip detector measurement (8 μm/pixel). The agreement between the two measurements, however, suggests that using multiple cameras to determine the 3D particle position results in better accu-

TABLE I.   Parameters of the experiments. u' is the root-mean-square velocity. ε is the turbulent energy dissipation rate per unit mass and is measured from the inertial-range scaling of the second order Eulerian velocity structure functions, as shown in [27]. The Taylor microscale Reynolds number is then defined as $R_\lambda \equiv (15u'^4/\varepsilon\nu)^{1/2}$. $L \equiv u'^3/\varepsilon$ is the integral length scale. η and τ_η are the Kolmogorov length and time scales, respectively. N_f is the frame rate of the cameras, in frames per τ_η. The measurement volume is nearly a cube in the center of the tank, and its lateral size is given in the units of η. Δx is the spatial discretization of the recording system. The spatial uncertainty of the position measurements is roughly $0.1\Delta x$. N_s is the total number of acceleration measurements.

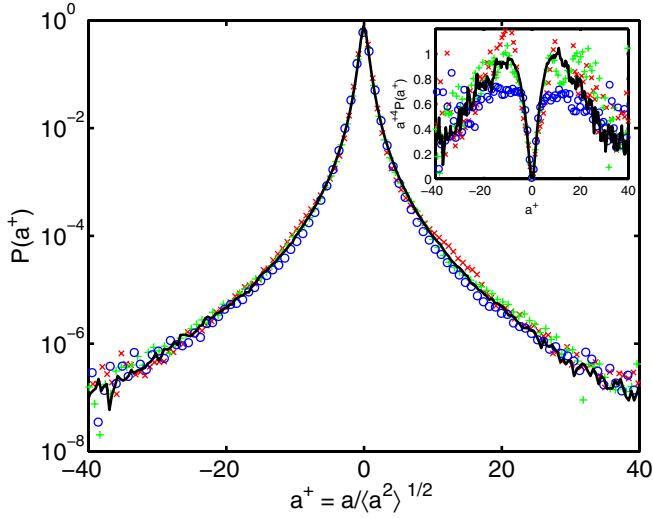| R_λ	u' (m/s)	ε (m²/s³)	L (mm)	η (μm)	τ_η (ms)	N_f (frames/τ_η)	meas. vol. (η^3)	Δx (μm/pix)	N_s
200	0.035	7.2×10^{-4}	61	194	37	37	$100 \times 100 \times 100$	80	2.5×10^7
350	0.11	2.0×10^{-2}	67	84	7.0	35	$300 \times 300 \times 300$	50	9.0×10^7
460	0.25	0.28	56	43	1.9	69	$240 \times 240 \times 240$	40	3.3×10^7
690	0.42	1.2	62	30	0.90	24	$670 \times 670 \times 670$	80	8.5×10^7

(a)

(b)

FIG. 1 (color online). Measured standardized acceleration $a^+ \equiv a/\langle a^2 \rangle^{1/2}$. The symbols are data from the LPT experiment at $R_\lambda = 460$: $\times$ and $+$ are the two measurements of the radial component, and $\bigcirc$ are the axial component of acceleration. The solid lines are the previous measurement of the radial component of acceleration using silicon-strip detectors in the same apparatus at $R_\lambda = 690$ [28]. The inset shows $a^{+4}P(a^+)$, the PDF of a^+ weighted by a^{+4}.

racy than the one-dimensional silicon-strip detector measurements.

Since we follow the motion of $O(10^2)$ tracer particles at a time, we can obtain Eulerian statistics from the cloud of particles (and their velocities and accelerations) at any instant. In Fig. 2, we compare the longitudinal and transverse acceleration correlation coefficients measured at different R_λ with the Obukhov-Yaglom predictions, as obtained from Eqs. (2). It can be seen from Fig. 2(a) that the predictions agree well with the experimental data. As R_λ increases, the agreement between the predictions and the measurements increases. This is not surprising given that the viscous contribution to acceleration is neglected in the theoretical predictions.

At large separations, the predicted acceleration correlations approach simple asymptotic scaling laws [15]:

$$R_{LL}(r) \approx \frac{2C_2^2}{9} \varepsilon^{3/2} \nu^{-1/2} (r/\eta)^{-2/3}, \qquad (6)$$

$$R_{NN}(r) \approx \frac{2C_2^2}{3} \varepsilon^{3/2} \nu^{-1/2} (r/\eta)^{-2/3}. \qquad (7)$$

Figure 2(b) compares Eqs. (6) and (7) with experimental data. There are small but appreciable discrepancies between the prediction and the measurements, which may be caused by the finite measurement volume and/or may reflect the need for still larger separations to see the asymptotic behavior. Another possible reason for the discrepancy is that our flows are not isotropic. We observe anisotropy in acceleration even at the largest R_λ investigated, although the anisotropy decreases with increasing R_λ [4].
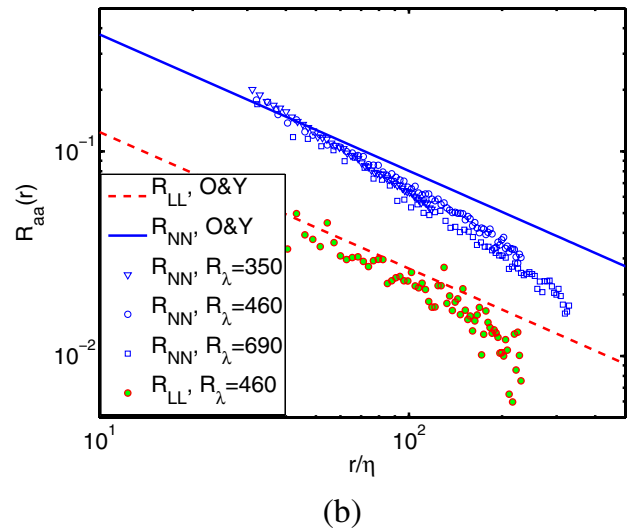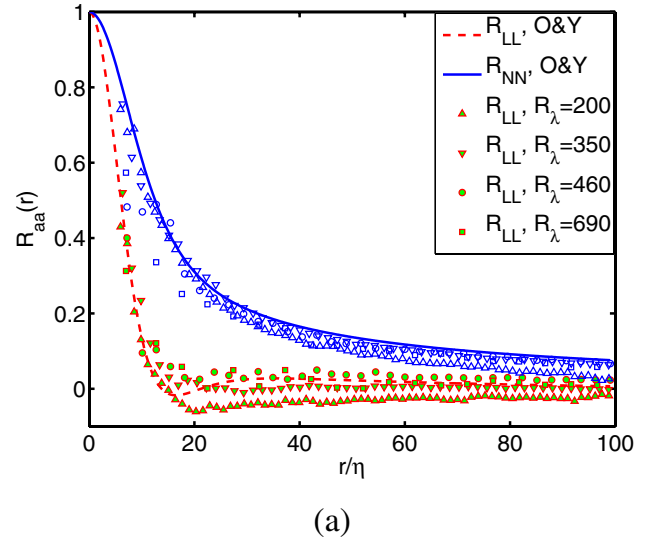
FIG. 2 (color online). Comparison of the measured acceleration correlation functions with the Obukhov-Yaglom prediction [15] for (a) small separations and (b) large separations. The dashed and solid lines are the predicted longitudinal and transverse correlation functions, respectively. The symbols correspond to measurements from LPT data at different Reynolds numbers. Filled symbols are R_{LL} and open symbols are R_{NN}. $\triangle$—$R_\lambda = 200$, $\triangledown$—$R_\lambda = 350$, $\bigcirc$—$R_\lambda = 460$, and $\square$—$R_\lambda = 690$.

We obtain $\Pi(r)$ by numerically integrating the experimentally measured $R_{NN}(r)$ using Eq. (2). As already mentioned before, this equation holds in homogeneous, isotropic turbulence at high-Reynolds numbers where the viscous contribution vanishes.

In Fig. 3, we compare the Obukhov-Yaglom prediction obtained from Eqs. (3)–(5) with measurements obtained from the acceleration correlations. We plot the normalized pressure structure function $D_p(r) \equiv \Pi(r)/\rho^2 \nu\varepsilon$. The measured data and the predictions are in good agreement over the range of separations accessible in the experiments. $K41$
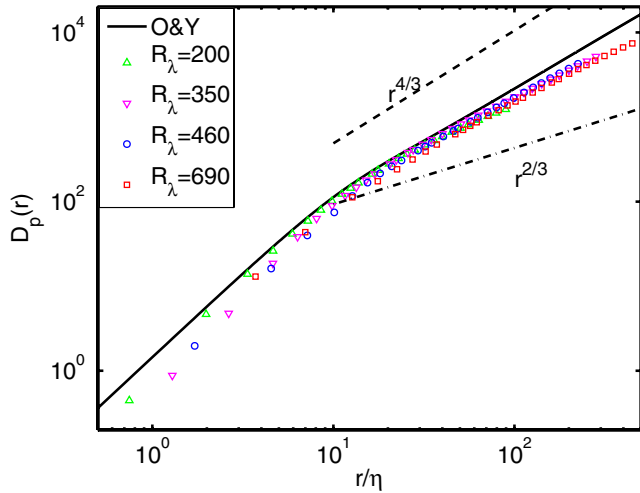
FIG. 3 (color online).   Comparison of the measured pressure structure functions with the Obukhov-Yaglom prediction [15]. The solid line is the prediction, and the dashed and dash-dotted lines indicate the $r^{4/3}$ and $r^{2/3}$ power laws, respectively. The symbols are measurements from LPT data at different R_λ: $\triangle$— $R_\lambda = 200$, $\bigtriangledown$—$R_\lambda = 350$, $\bigcirc$—$R_\lambda = 460$, and $\square$—$R_\lambda = 690$.

inertial-range scaling can be obtained from the limiting case of $r \gg \eta$ in the prediction of $\Pi(r)$, yielding $D_p(r) \sim (r/\eta)^{4/3}$, which is also plotted in Fig. 3. This scaling law is close to the experimental data in the inertial-range. For comparison, the $r^{2/3}$ scaling law, as suggested by previous simulations at relatively low R_λ [5,12,18], is also shown in Fig. 3. As can be seen, all experimental data are much closer to the $K41$ scaling rather than $r^{2/3}$ scaling, and there is no appreciable change of slope over the range of $200 \lesssim R_\lambda \lesssim 690$. As shown for the case of Lagrangian velocity [30], the extent of the nominal inertial range measured from the spectrum or from the structure function can be very different. This subtlety could account for the difference between our experimental results and previous investigations, in which the pressure spectra were studied.

In summary, we simultaneously followed the trajectories of multiple passive tracer particles in turbulent water flows with $200 \lesssim R_\lambda \lesssim 690$. The accuracy of the accelerations measured from the trajectories is comparable to previous single-particle measurements. We obtained spatial acceleration correlations from the multiparticle measurement and used the measured acceleration correlations to compute pressure structure functions from a relation that holds at high-Reynolds numbers. We compared the measurements with theoretical predictions by Obukhov and Yaglom [15] and found that the predictions of both the acceleration correlations and the pressure structure functions are in good agreement with the experimental data. We also observed $K41$ inertial-range scaling in the measured pressure structure functions over the range of Reynolds numbers investigated.

We thank J. Bec for helpful discussions and J. Mann for bringing Ref. [15] to our attention. This work was sup-

*Present address: Department of Physics, Haverford College, Haverford, PA 19041, USA.
†eberhard.bodenschatz@ds.mpg.de
[1] P. K. Yeung, Annu. Rev. Fluid Mech. **34,** 115 (2002).
[2] R. A. Shaw, Annu. Rev. Fluid Mech. **35,** 183 (2003).
[3] G. A. Voth, K. Satyanarayan, and E. Bodenschatz, Phys. Fluids **10,** 2268 (1998).
[4] A. La Porta *et al.*, Nature (London) **409,** 1017 (2001); G. A. Voth *et al.*, J. Fluid Mech. **469,** 121 (2002).
[5] P. Vedula and P. K. Yeung, Phys. Fluids **11,** 1208 (1999).
[6] L. Biferale *et al.*, Phys. Rev. Lett. **93,** 064502 (2004).
[7] P. K. Yeung *et al.*, Phys. Fluids **18,** 065103 (2006); P. K. Yeung *et al.*, J. Fluid Mech. **582,** 399 (2007).
[8] N. Mordant, A. M. Crawford, and E. Bodenschatz, Phys. Rev. Lett. **93,** 214501 (2004); A. M. Crawford, N. Mordant, and E. Bodenschatz, Phys. Rev. Lett. **94,** 024501 (2005).
[9] S. Ott and J. Mann, J. Fluid Mech. **422,** 207 (2000).
[10] B. Lüthi, A. Tsinober, and W. Kinzelbach, J. Fluid Mech. **528,** 87 (2005).
[11] N. T. Ouellette, H. Xu, and E. Bodenschatz, Exp. Fluids **40,** 301 (2006).
[12] J. Bec *et al.*, Phys. Rev. Lett. **98,** 084502 (2007).
[13] M. Ould-Rouis *et al.*, Phys. Rev. Lett. **77,** 2222 (1996).
[14] A. N. Kolmogorov, Dokl. Akad. Nauk SSSR **30,** 301 (1941) [Proc. R. Soc. A **434,** 9 (1991)].
[15] A. M. Obukhov and A. M. Yaglom, Prikl. Mat. Mekh. **15,** 3 (1951) [National Advisory Committee for Aeronautics Report No. TM-1350, 1953.]
[16] A. S. Monin and A. M. Yaglom, *Statistical Fluid Mechanics* (MIT Press, Cambridge, MA, 1975), Vol. 2.
[17] R. J. Hill and O. N. Boratav, Phys. Rev. E **56,** R2363 (1997).
[18] T. Gotoh and D. Fukayama, Phys. Rev. Lett. **86,** 3775 (2001).
[19] Y. Tsuji and T. Ishihara, Phys. Rev. E **68,** 026309 (2003).
[20] A. M. Yaglom, C. R. Akad. URSS **67,** 795 (1949).
[21] M. D. Millionshichkov, Dokl. Akad. Nauk SSSR **32,** 611 (1941).
[22] W. Heisenberg, Z. Phys. **124,** 628 (1948).
[23] T. de Kármán and L. Howarth, Proc. R. Soc. A **164,** 192 (1938).
[24] S. B. Pope, *Turbulent Flows* (Cambridge University Press, Cambridge, England, 2000).
[25] K. R. Sreenivasan, Phys. Fluids **7,** 2778 (1995).
[26] M. Bourgoin *et al.*, Science **311,** 835 (2006); H. Xu *et al.*, Phys. Rev. Lett. **96,** 024503 (2006).
[27] H. Xu *et al.*, in *Advances in Turbulence XI: Proceedings of the 11th EUROMECH European Turbulence Conference*, edited by J. M. L. M. Palma and A. Silva Lopes (Springer, New York, 2007), pp. 1–10.
[28] N. Mordant, A. M. Crawford, and E. Bodenschatz, Physica (Amsterdam) **193D,** 245 (2004).
[29] L. Chevillard *et al.*, Phys. Rev. Lett. **91,** 214502 (2003).
[30] R.-C. Lien and E. A. D'Asaro, Phys. Fluids **14,** 4456 (2002).